

Summary of the Interaction of a Rotor Wake with a Circular Cylinder

J. M. Kim* and N. M. Komerath†

Georgia Institute of Technology, Atlanta, Georgia 30332

To compute the aerodynamics of a rotorcraft in low-speed flight, the interaction of the strong vortices in the rotor wake with the airframe must be modeled. Using a hemisphere-cylinder airframe and a two-bladed rotor for reference, the various phenomena encountered during such interactions are summarized, combining previous results on various configurations with recent experimental results. Differences between the interaction at the front and aft portions of the wake are discussed. The precollision phase conforms to expectations from potential flow, and includes distortion of the vortex trajectory determined by the sense of rotation of the vortex. The collision phase involves complex boundary-layer interactions. The axial velocity in the vortex core causes substantial asymmetry and influences the surface pressure distribution on the airframe side under the advancing rotor blade, where the axial flow stagnates. The postinteraction vortex is much weaker, but still contains some swirl energy. Where flow separation occurs due to airframe shapes, the interaction is not modified significantly, because the vortex dominates the interaction with separated shear layers for parameter values of practical interest. Areas of remaining uncertainty are discussed.

Nomenclature

$C_{P_{inst}}$	$= (P_{inst} - P_{\infty})/q_{\infty}$
H	$=$ vertical spacing between rotor hub center and airframe centerline
P_{inst}	$=$ instantaneous static pressure
q_{∞}	$=$ freestream dynamic pressure
R	$=$ rotor radius
U_{∞}	$=$ tunnel freestream velocity
X	$=$ distance parallel to tunnel axis from rotor hub center
Z	$=$ vertical distance from rotor hub center
μ	$=$ rotor advance ratio, $U_{\infty}/\Omega R$
ϕ	$=$ circumferential location of points on the surface of the airframe cylinder, measured from the top of the airframe
Ψ	$=$ rotor azimuth measured from downstream position, deg
Ω	$=$ rotor angular velocity

Introduction

WHEN a rotorcraft hovers or flies at low speed, the wake of its rotor interacts with the airframe. The wake is dominated by strong tip vortices. Since these vortices remain in the vicinity of the vehicle, they have a profound influence on the velocity field and on rotor loads and fuselage surface pressure distributions. Modern schemes to calculate rotor aerodynamics either specify the trajectory of the vortices or let the wake evolve in a force-free manner. When an airframe is immersed in the rotor wake, prediction of the behavior of the vortices becomes extremely difficult for want of firm physical understanding verified by observation. This is the genesis of the work summarized in this paper: the search for a definition and understanding of the behavior of a rotor vortex system around an airframe. We summarize efforts over the past eight years conducted at this laboratory and complete the picture using recently obtained results from here and elsewhere. We emphasize that the objective is to provide a perspective on the problem to guide aerodynamics prediction and acknowledge that there are intricate phenomena still to be explored.

Presented as Paper 93-3084 at the AIAA 24th Fluid Dynamics Conference, Orlando, FL, July 6-9, 1993; received July 7, 1993; revision received April 4, 1994; accepted for publication April 19, 1994. Copyright © 1994 by J. M. Kim and N. M. Komerath. Published by the American Institute of Aeronautics and Astronautics, Inc., with permission.

*Graduate Fellow, School of Aerospace Engineering; currently with Korean Aerospace Labs.

†Professor, School of Aerospace Engineering. Associate Fellow AIAA.

The Georgia Institute of Technology (GT) model¹ is used to focus discussion. Designed for simplicity of analysis and efficiency of pressure measurement, it consists of a pressure-instrumented circular cylinder with a hemispherical nose, mounted at variable heights below a one-piece, two-bladed rotor which is held in a simple teetering hub. At the aft end, the cylinder extends far downstream of the rotor. The rigid NACA 0015 rotor blades are fixed at 10-deg collective pitch, but the rotor tip path orientation varies with the test conditions. The University of Maryland (UMD) model² is another on which studies have been performed. Designed to be more representative of existing rotorcraft, it has a four-bladed rotor with fully articulated hub, mounted on a pressure-instrumented hemisphere/cylinder, tapering to a boom of smaller diameter downstream.

Figure 1 shows three views¹ of the wake as it approaches the GT cylinder, at an advance ratio μ of 0.1. The figure was constructed as follows: a laser sheet, successively aligned in each of the many vertical and horizontal planes, was strobed at a frequency close to that of the rotor. The tunnel was seeded uniformly with a mineral oil fog. The vortex core cross section was visible in the sheet as a dark region devoid of seed particles. The motion of the core was thus seen in slow motion on video, with the frames corresponding to blade passage through the sheet also identifiable for phase reference. Frames were frozen in succession on a television monitor on which core positions were marked and transferred manually to an overlaid graph paper. This procedure yielded the trajectories shown in Fig. 1. A skewed-cylinder rigid wake model would have given circular arcs matched to these trajectories away from the cylinder. Distortion of the real trajectory is evident near the cylinder. The trajectory at the front of the wake appears decelerated. This corresponds to expectations based on the sense of rotation of the vortex and image plane models of vortex/surface interactions found in texts on potential flow. In these early experiments, it was impossible to discern the vortex core very near or below the cylinder. It did appear that the broken end under the retreating-blade side (RBS) moved rapidly along the filament away from the cylinder. Beyond identifying the distortion, definite guidance could not be obtained regarding vortex behavior around the cylinder.

Previous Studies

Lorber and Egolf³ studied the complex aerodynamics of wake/fuselage interaction, comparing their results to the data in Refs. 1 and 4 on the GT model. Starting with the United Technologies Research Center (UTRC) generalized wake, they achieved successful semiquantitative predictions (peaks underpredicted) of unsteady pressures on the cylinder top surface. Close to the cylinder,

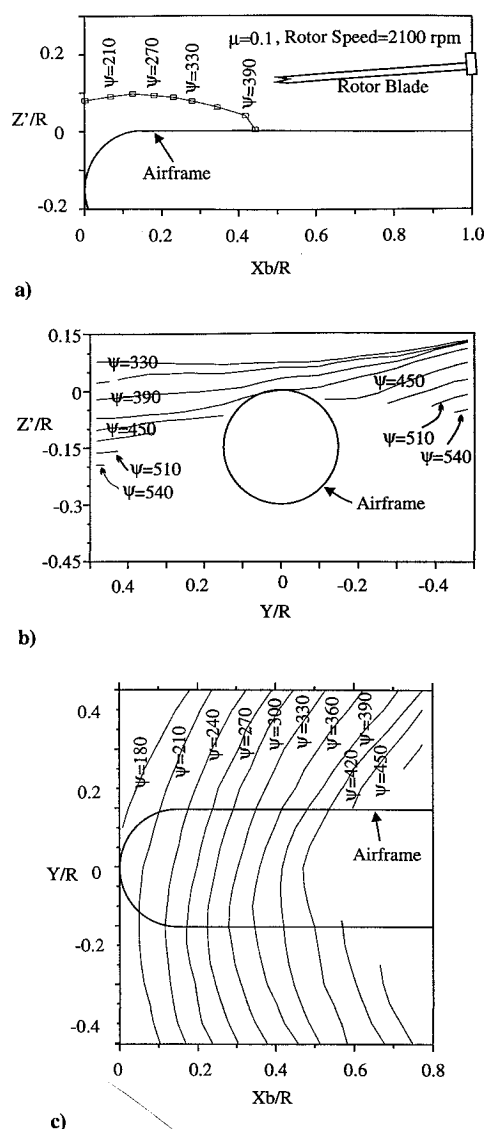


Fig. 1 Vortex trajectories over the GT model, from Ref. 1.

they forced the vortex system to stay outside a specified boundary concentric with the cylinder. They identified the vortex/body interaction as the major uncertainty in computing the rotor/fuselage interaction. Quackenbush and Bliss⁵ developed an analytical technique to handle the dynamics of close vortex-surface interaction. A fat-core model of the vortex was used close to the airframe surface, primarily to avoid velocity discontinuities. An asymptotic procedure matched this model to the external free wake. The authors of Ref. 5 were able to predict the distortion of the trajectory for a geometry corresponding to the aft edge of the wake over a cylinder. Here the vortex filament was shown to be accelerated downstream, so that the vortex would appear to skim over the surface for some distance, as shown schematically in Fig. 2. Once the vortex collided with the airframe, it was not possible to predict subsequent wake behavior. Figure 2 is discussed at length later.

Some curious vortex/surface interactions were documented by Norman and Light⁶ using wide-field shadowgraphy in a full-scale rotor test. The tip vortices were seen to interact strongly with the supports of the rotor system. Liou et al.⁷ performed detailed experiments on the interaction of the tip vortex with the top of the Georgia Tech (GT) model, measuring the azimuth-resolved velocity field and the surface pressure variation in the region of vortex impingement and correlating these with flow visualization results. Using contours of the lateral component of vorticity and surface pressure data, he was able to obtain a clear definition of the distortion of the core, the occurrence of high stagnation pressures, as well as the sharp pressure drop characteristic of vortex interaction. Most curi-

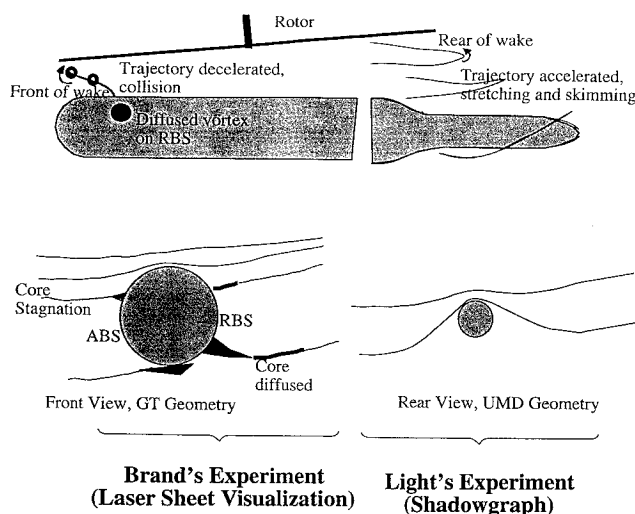


Fig. 2 Summary of vortex behavior around a cylinder, based on observations for the GT model (front part) and the UMD model (aft part).

ous of these features was one showing a half-vortex with a velocity profile and vorticity distribution conveying the impression that the bottom half of the vortex disappeared into the airframe surface boundary layer although the top half remained almost unchanged. Several other observed features remained unexplained. Two of these were a large secondary vortical structure of opposite circulation that appeared downstream of the region where the tip vortex collided and a small secondary vortical structure that appeared upstream of the tip vortex just prior to collision in the vorticity contours. On the RBS, a weaker tip vortex structure was visible from velocity data in the region where the flow visualization of Ref. 1 had discerned no particle deficit. At the time of the experiments of Liou et al.⁷ there was little guidance on what to observe in greater detail. There was no motivation to study the details of the collision process, for example.

Mavris et al.⁸ were able to see the effects of the vortex interaction on the performance of a prediction code. Two approaches were tried. First, the energy addition to the flow through the rotor disk was modeled by dividing the disk into sectors of annular rings. This energy was then assumed to convect down the skewed wake. The resulting increase in stagnation pressure was superposed all around the cylinder as a time-averaged effect, after computing the rotor-airframe interaction using a combination of Scully's free wake⁹ and the VSAERO surface panel code.¹⁰ This model, however ad hoc, proved to be remarkably successful in computing the measured pressure distribution over the top and sides of the cylinder. Encouraged by this success, the computational scheme¹¹ was refined, including an unsteady potential term after the work of Ref. 2. By this time, detailed velocity measurements⁷ over the top and RBS of the cylinder had become available, as had the azimuth-resolved pressure measurements around the cylinder of Ref. 1. The results were surprising. Although agreement with experiment was excellent along the top of the cylinder, there were obvious problems along the sides. It was clear that things were happening as modeled by the potential flow code until the vortex collided with the cylinder. After that, the predicted and measured trends of surface pressure were opposite, and this disagreement propagated down the sides of the cylinder on the RBS, following the vortex interaction trajectory. When the measured periodic velocity field from Ref. 7 was used in the computation instead of that computed from the singularity strengths, the agreement in surface pressure on the RBS improved substantially. It was clear that the velocity field after vortex-surface interaction could not be computed without more detailed knowledge.

In mid 1988, the state of knowledge¹² was that the approach of the vortex system to the airframe could be modeled with confidence using potential-flow concepts. The distortion of the filaments in the vicinity of the airframe could be predicted, with accuracy limited only by the knowledge of the vortex strength and structure. Once the collision with the surface began, uncertainties mounted, and

nothing could be predicted about the behavior of the vortex system or the surface flowfield beyond this stage. For many aspects of rotorcraft aerodynamics, this was a major advance: the rotor loads are primarily affected by the first 360 deg of the vortex trajectory. The pressure fluctuations are most violent along the spine of the airframe, and these could be predicted with excellent fidelity.

More recently, experiments using wide-field shadowgraphy at the University of Maryland¹³ showed images that could be explained using the Quackenbush and Bliss model⁵ (see also Ref. 12). The "skimming" motion of the vortex over the airframe over the aft portion of the airframe appears quite clear. Without depth perception or a way of viewing from downstream, the behavior of the vortex system very close to and around the airframe remained uncertain.

Issues

For several other aspects of rotorcraft aerodynamics, this state of knowledge left major gaps unfilled. Blade-vortex interaction phenomena are highly sensitive to vortex trajectories; minor influences due to the fuselage, tail boom, and distortion of later turns of the vortex system could make a major impact. Tail boom flowfields have become extremely important in recent years because of tail rotor loads and noise and designs which eliminate the tail rotor. The behavior of the vortex system on interaction with the separated flow downstream of the rotor mast and around the sides of the fuselage remained unknown. The major issues were 1) the filament structure on either side of the cylinder as the vortex moves down the sides, whether filaments get cut, and if so, what happens in the broken region and at the cut ends; 2) what happens below the airframe; 3) the physics of vortex-surface collision, at arbitrary orientations, specifically in predicting surface pressure variations, severity, time scales, and directions of pressure gradients, and the importance of viscous effects; 4) vortex-induced boundary-layer separation; 5) the interaction of strong vortices with separated-flow regions; and 6) the impact of the axial velocity in the core.

Recent work has attempted to answer some of these questions. The computations of Mavris et al. depended on the periodicity of the wake to predict unsteady surface pressure and velocity over the cylinder. Berry¹⁴ and Schreiber¹⁵ made progress on the problem without assuming periodicity. Berry developed a potential flow method with a time-stepping finite difference approach. The fuselage was modeled as a nonlifting body of source panels, and the rotor and wake were modeled by a full vortex lattice. Schreiber used a Lagrangian vortex "cloud" approach, developed from the work of Cantaloube and Huberson.¹⁶ Schreiber combined the modified vortex particle model with a boundary element computation for bodies in relative motion. An unsteady formulation was used to solve an initial value problem for the transport of vorticity in time and a boundary value problem for the induced velocity field within the framework of an ideal flow model. Schreiber's code thus could compute the rotor/airframe interaction in a completely unsteady manner, whereas Mavris et al. used a periodic approach to add on the blade passage effect.

Both Schreiber and Berry achieved fair measures of success. In Berry's case, the geometry of the tip vortex trajectory (before close approach to the cylinder) and the wake effects on rotor inflow were successfully calculated. Difficulties were encountered in computing surface pressure, including the substantial effects of the vortex, and no comparisons with experiment were demonstrated. In Schreiber's case, the vortex trajectory and surface pressure distribution were calculated with a fair degree of success, and showed the blade passage effects on the fuselage and rotor blade surface pressure in a dynamic manner. Pressure effects of vortex proximity could also be seen. However, the vortex cloud diameter required to ensure stability of the Lagrangian procedure became far too large to be used in studying vortex-surface interaction. The magnitudes of vortex-induced pressure changes on the surface did not compare well with experiment. Both approaches thus succeeded in predicting the vortex trajectory until severe surface interaction commenced. Clark and Maskew¹⁷ have developed an unsteady wake distortion scheme, applied to the UMD geometry. No results appear to have been published for cases of strong vortex/airframe interaction.

Experiments by Brand et al.¹⁸ correlated the vortex trajectory

with detailed surface pressure variations on top of the GT cylinder. A sliding key carrying flush-mounted microphones was moved in small steps along a special section of the cylinder to obtain fine spatial resolution. This provided the phase-resolved pressure as the blades moved across the surface and the vortex approached and collided with the surface. The results were animated by videotaping 60 plots of the vortex location and the instantaneous pressure distribution. This dynamic data set again showed the secondary feature downstream of vortex impingement observed by Liou et al.⁷

Recent work has proceeded along two avenues. One is the detailed examination of the collision process. Conlisk¹⁹ computed the pressure field during a vortex/boundary-layer interaction and showed the development of severe pressure gradients. Initially motivated by the vortex/boundary-layer interaction in turbulent boundary layers,²⁰⁻²² this opened the way to examine a tip vortex/surface interaction in detail. Affes and Conlisk²³ extended this work to vortex interaction with curved surfaces. Given the initial vortex positions, core radius, estimates of vortex circulation, and velocity field data of the GT configuration, they computed the position and magnitude of the suction peak on the surface due to vortex proximity (in the precollision stage), obtaining excellent agreement with the GT experiments. Recently Affes et al. also computed the onset of boundary-layer separation, including the viscous interaction by solving the three-dimensional unsteady boundary-layer equations. The computation was continued to examine the three-dimensional boundary layer as well as events along the RBS. This predicted the initiation and development of a secondary separation region of opposite vorticity upstream of the tip vortex just before the core collided with the surface. A focused experiment succeeded in capturing this phenomenon. At this writing, it appears that the vortex core structure is essentially unmodified until it is about one core diameter above the top of the GT cylinder, but boundary-layer separation is initiated and a secondary recirculation region forms upstream. Following this, the impingement phase begins, which has not yet been studied in detail either experimentally or numerically. In Ref. 25, predictions of vortex behavior are made for the geometries of both the GT and UMD models.

Experiments have continued in parallel, seeking an overall picture of the interaction around the cylinder. This is the new work presented in this paper. A pulsed copper vapor laser has enabled much better visualization that what was possible with the continuous-wattage argon laser. Figure 3 shows vorticity contours measured by Liou et al.⁷ during the precollision phase above the airframe with vortex core images. As the core begins to distort, a large region of opposite vorticity appears below the vortex. Figure 2 attempts to show the differences between the interaction at the front and rear edges of the wake. A combination of the GT and UMD model geometries is used for illustration. The approach to the top of the cylinder is similar in both cases in that the filament is perpendicular to the cylinder axis. In the GT case, the filament trajectory bends downward and forward as it descends to the surface. Brand et al.¹ argued that the filament must break in two due to the diffusion occurring during interaction with the boundary layer. No vortex structure could be identified beneath the cylinder. Light et al.¹³ indicated that the filament wraps around the cylinder as it convects downstream and is visible below the cylinder. The interaction at the aft edge of the wake as in Ref. 13 is more amenable to potential-flow modeling because the distortion can be interpreted excluding viscous effects. An example is Ref. 5.

Some differences between the two cases follow. In the Ref. 1 experiment at the front of the wake, the sense of rotation of the vortex is such that downstream motion is retarded, and the vortex collides quickly with the cylinder. Recent experiments²⁴ have shown more details about the collision process, but it still appears that after collision, the vorticity of the tip vortex adds and merges with the vorticity of the boundary layer. In contrast, the vortex at the aft portion of the cylinder is accelerated downstream. It thus slides above and parallel to the surface. In addition, the larger cylinder radius in the Ref. 1 experiment ($0.3R$) causes diffusion over a wider segment of the vortex than in Ref. 13 ($0.12R$). The apparent filament wrap-around in Ref. 13 appears to occur when the parts of the filament on either side of the airframe continue downward while the filament above the airframe slides downstream. Substantial filament stretching must occur in this case, as predicted in Ref. 23. The signs of the

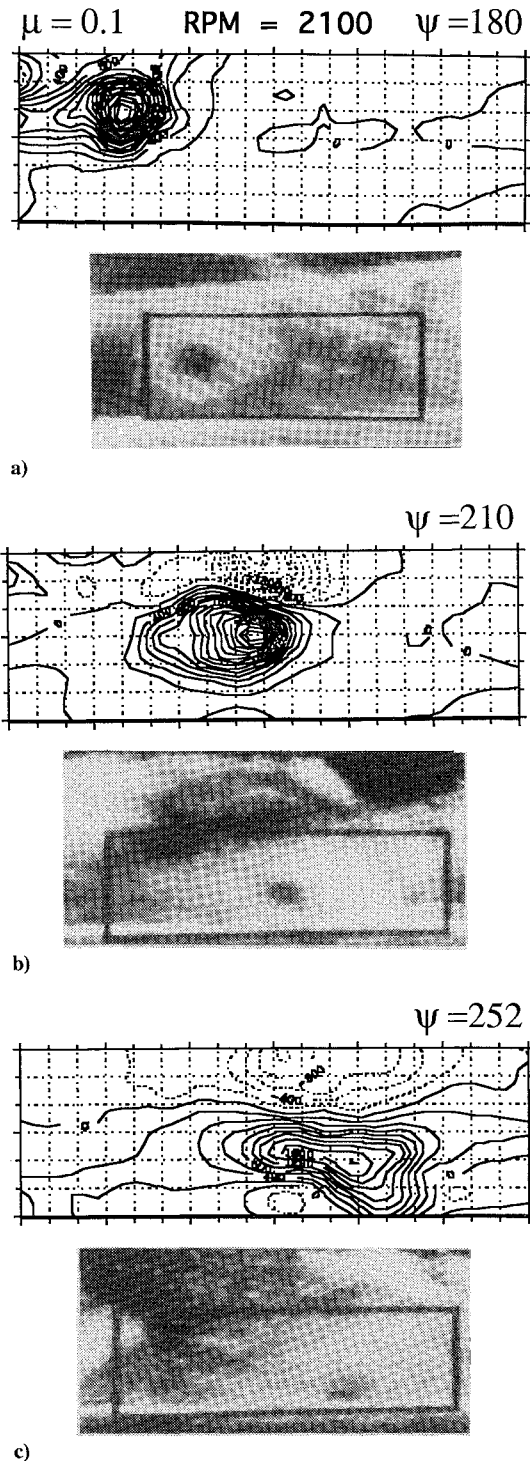


Fig. 3 Contours of the lateral component of vorticity from Ref. 7 compared with vortex core cross-sectional images acquired by Kim²⁷ in the vertical plane through the GT cylinder axis.

vorticity of the filament and the boundary layer are opposite. There is no evidence of the filaments on the sides actually coming closer to the airframe or reconnecting below it; note that shadowgraphy does not resolve depth.

New Experiments

A key feature of the rotor tip vortex is the substantial axial velocity along the core. Unlike unburst delta-wing vortices, this core is wake-like i.e., the flow inside the core moves toward the blade that left the vortex behind. Thompson et al.²⁶ reported axial velocities of the same order as the maximum tangential velocity in the core of a rotor tip vortex in hover within the first 180 deg of vortex age. For the GT configuration, Liou et al.⁷ reported axial velocities compara-

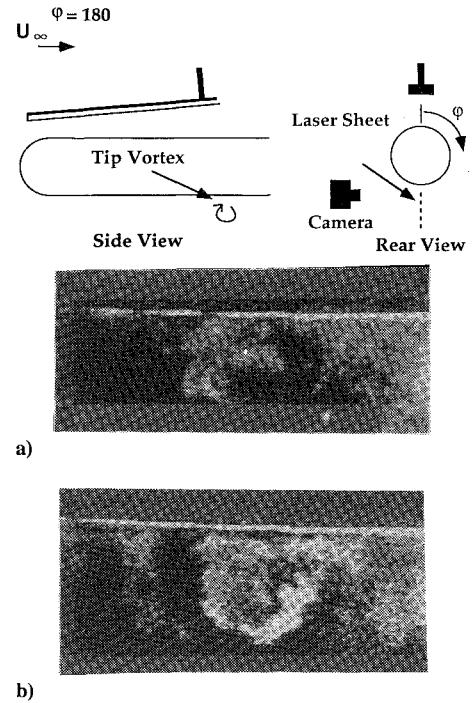


Fig. 4 Pulsed laser sheet images (digitally-enhanced) of the tip vortex below the GT cylinder.

ble to the rotor inflow velocity for vortex ages above 360 deg. This velocity determines much of the interaction around the airframe. In particular, we note the following aspects, before presenting detailed evidence. The vortex filament resembles a tube containing a helical flow, following the rotor blades across the cylinder from the advancing-blade side (ABS) to the RBS. Thus, the axial flow should stagnate on the ABS and cause suction on the RBS. In addition, under the cylinder, the axial component causes the remaining helical flow to cross the plane of symmetry to the RBS. Evidence is presented in the following.

Visualization of the Vortex Below the Cylinder

With the enhanced pulse intensity and temporal resolution of the light sheet from a copper vapor laser, combined with an intensified camera, it was possible to examine the vortex behavior below the GT cylinder. Figure 4 shows two images of the vortex below the cylinder ($\Phi = 180$ deg), captured during two consecutive rotor revolutions at the same blade azimuth. However, when the light sheet was moved more toward the RBS, this structure was not identifiable. This is discussed later in the context of the surface pressure distribution.

Visualization of Core Stagnation

Vertical and horizontal cross sections of the wake were studied using laser sheets. Vertical planes were visualized using the copper vapor laser. Horizontal planes immediately above the cylinder were visualized using a sheet from an argon ion laser, strobed using a Bragg cell. Although the light intensity was much lower than that of the copper laser, this was the only way to produce sheets thin enough to precisely illuminate sections immediately above the surface, cutting along the core of the filament. The objective was to discern the core using its particle deficit. Images from the vertical plane at the RBS ($\Phi = 270$ deg) are shown in Fig. 5. Figure 5a shows a clear particle void in the vortex core where the filament has not yet reached the surface at the top of the cylinder. In Fig. 5b, slightly later in rotor azimuth, the filament has already suffered interaction with the surface at the top. The particle void has disappeared, but the vortical motion is still clearly visible. Figure 6a shows results from a horizontal laser sheet tangential to the top of the cylinder. The original images, from the argon laser, have too little contrast to be reproduced in a printed paper, so the vortex trajectory was traced over the digitized color image to produce this figure. The particle deficit in the core was clearly visible on the ABS but not visible on

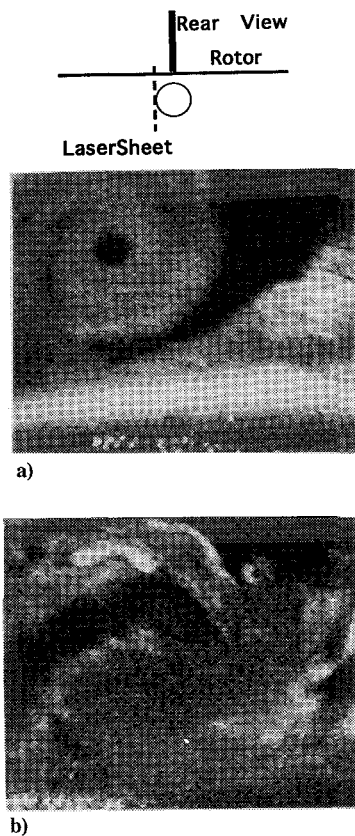


Fig. 5 Pulsed laser sheet image of the tip vortex core a) before and b) after interaction with the surface, showing the particle deficit disappearing after surface interaction occurs at the top of the GT cylinder.

the RBS. The void seems to expand just before contact with the top of the cylinder, showing a pattern reminiscent of vortex bursting on a delta wing. The axial flow in the core has stagnated. Figure 6b shows what happens when the laser sheet is moved 12.5 mm above the top surface. Here the particle deficit in the core is clearly visible as the filament sinks through the sheet, going across the cylinder. The distortion of the trajectory is also visible. This provides further proof of the stagnation of the axial flow in the core during interaction with the cylinder. Using this logic, we can presume that under the cylinder, the axial flow must therefore drive the vortex from the ABS into the plane of vertical symmetry of the cylinder, but not much beyond.

Pressure Distribution around the Cylinder

Figure 7a shows the surface pressure distribution along the top of the airframe ($\phi = 360$ deg) as a function of rotor azimuth Ψ , for the front portion of the airframe where the leading edge of the wake interacts. Three dominant features are visible. The highest peaks correspond to the pressure pulse felt as the pressure distribution around the lifting rotor blade moves across the airframe above the microphones. The deep oblique valleys correspond to the tip vortex interacting with the surface. This starts at about $Xb/R = 0.16$, when the blade azimuth is at 90 deg. The tip vortex age at this point is 270 deg, when the vortex is roughly 4 core diameters above the airframe as shown in Fig. 1. The suction peak can be seen until it is obscured by the blade passage effect at $\Psi = 180$ deg. The vortex-induced suction is greatest at $\Psi = 234$ deg, when an instantaneous pressure coefficient of -7.57 is reached. At this stage, the core is very close to (less than one core diameter from) the surface. By $\Psi = 348$ deg, the suction peak disappears. At this stage, the filament can be considered to be broken into two. The shallower valley is caused by the secondary feature earlier observed by Liou et al.⁷ and Brand et al.¹⁸ This has been shown by Kim^{27,28} to be caused by the interaction of the concentrated rollup at the edge of the inboard vortex sheet, which forms a vortical structure rotating counter to the tip vortex. The counter-rotating vortex (CRV) suction peak moves

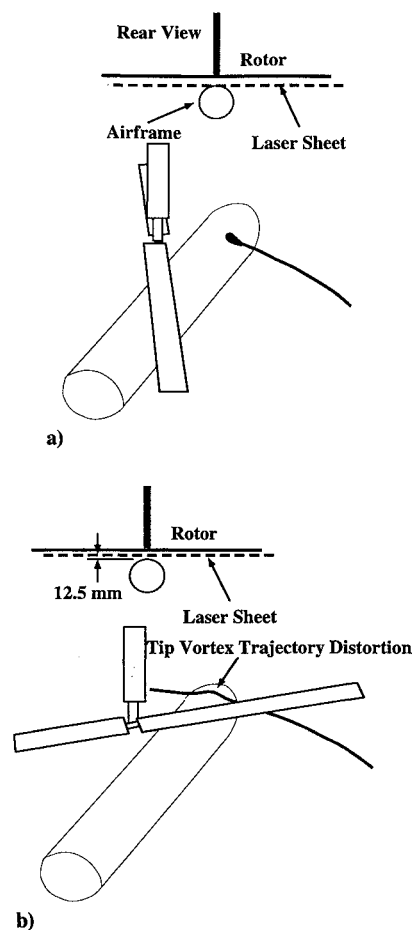


Fig. 6 Stagnation of axial flow during vortex interaction at the top of the GT cylinder, traced from argon ion laser sheet images; a) stagnation during interaction and b) distortion prior to interaction.

faster downstream than the tip vortex due to the difference in the sense of rotation between these two features.

The rest of Fig. 7 shows excerpts from Ref. 27 on the pressure distribution around the airframe. As we move from the top ($\Phi = 360$) to the RBS at $\Phi = 270$ deg, the longitudinal spacing between the suction peaks from the two different vortex features decreases. Between 270 and 285 deg, the two suction peaks meet at a certain blade azimuth, when the peak becomes sharp and high. Under the ABS, however, the two suction peaks never meet, and the peak magnitude remains low. It appears that on the RBS, the two adjacent vortices with different senses of rotation induce a higher downward velocity and a larger suction peak.

Under the cylinder ($\Phi = 180$ deg), the oblique suction valley appears similar to those at other circumferential locations. Recall that the vortex was seen in Fig. 4 below the cylinder, but conclusive proof could not be advanced on its genesis. Comparing suction peaks, the magnitude decreases going from $\Phi = 180$ to 195 deg, showing that the vortex visible at 180 deg comes from the ABS. Further, the suction on the ABS at $120 < \Phi < 165$ is greater than that at $195 < \Phi < 240$, again due to the asymmetry in the axial flow.

The pressure distribution on the cylinder, viewed at fixed values of rotor azimuth, is shown in Fig. 8. The vertical and horizontal axes in each contour plot represent circumferential and longitudinal coordinates on the cylinder surface, respectively. Since the measurement grid was optimized to visualize the vortex interaction, there are no pressure data in the rectangular regions left blank. Otherwise, lighter regions indicate higher pressures.

When the blade is aligned with the cylinder axis, the blade passage effect is seen at $\Psi = 360$ deg in Fig. 8a as a positive pressure concentration. As the blade moves to $\Psi = 30$ deg, the blade passage effect is seen as two positive pressure concentrations, disconnected by the tip vortex effect. This is also observed at $\Psi = 150$ deg. At $\Psi = 60$ deg, the low-pressure concentration due to the tip vortex

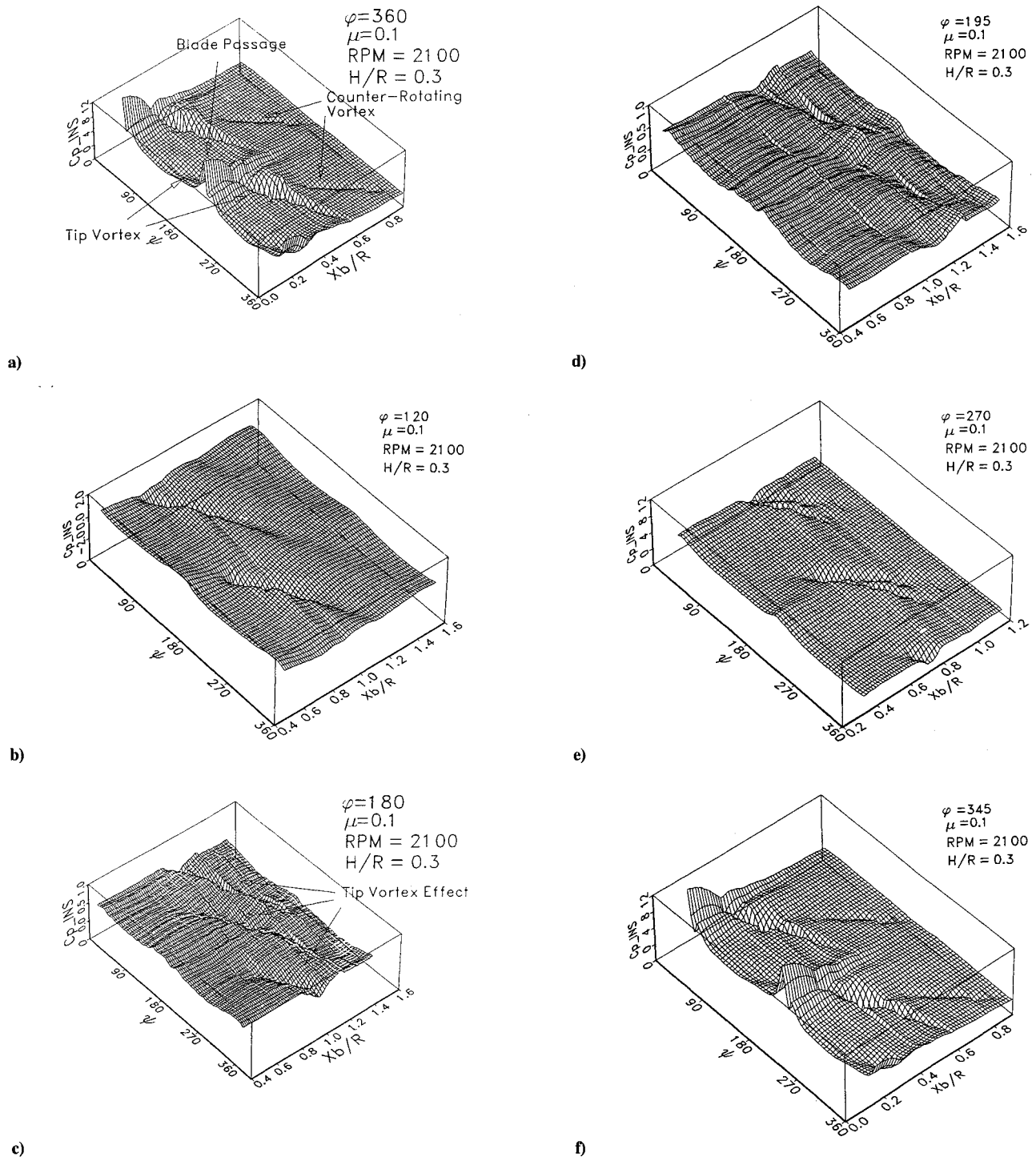


Fig. 7 Pressure distribution along the axis of the GT cylinder, as a function of rotor azimuth, for various positions around the cylinder azimuth.

splits into two, confirming the vortex filament cut observed in the flow visualization. These low-pressure regions then move downward and downstream. The tip vortex effect is felt somewhere on the cylinder surface for a period longer than 360 deg of blade rotation. For instance, in the contour at $\Psi = 60$ deg, three suction peaks are seen on both sides of the cylinder. The low-pressure regions on each side have an interval of 180 deg in rotor azimuth. The pressure concentration on the ABS survives until it reaches the cylinder bottom, whereas on the RBS it disappears at about $\Phi = 240$ deg.

Geometry of the Vortex Stagnation

As previously noted, a positive pressure concentration is observed on the cylinder surface at a location close to a low-pressure region

on the ABS for rotor azimuth $30 < \Psi < 120$ deg. Figure 9 shows a surface pressure contour at $\Psi = 72$ deg and the corresponding longitudinal pressure distribution at $\Phi = 30$ deg, where a strong tip vortex effect is observed. Note that the strong positive peak is present only downstream of the suction peak in the longitudinal surface pressure distribution. This positive peak appears to be caused by the axial component of velocity in the tip vortex. Then a question is raised: why is the axial flow effect exhibited only downstream of the tip vortex suction peak? The asymmetry in the pressure distribution can be explained by combining the axial and circulatory motion of the tip vortex filament. The schematic diagram in Fig. 10 shows the axial velocity component stagnating near the top of the airframe (based on flow visualization) and a vortical flow with an axial component of velocity interacting with the airframe surface. When the

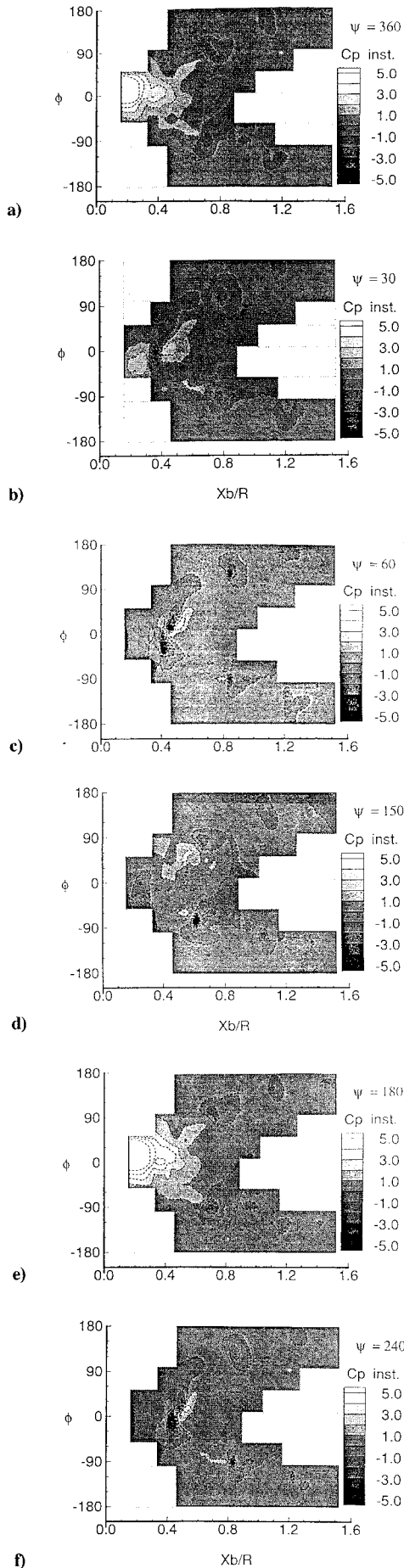


Fig. 8 Pressure distribution around the cylinder, viewed at several discrete values of rotor azimuth.

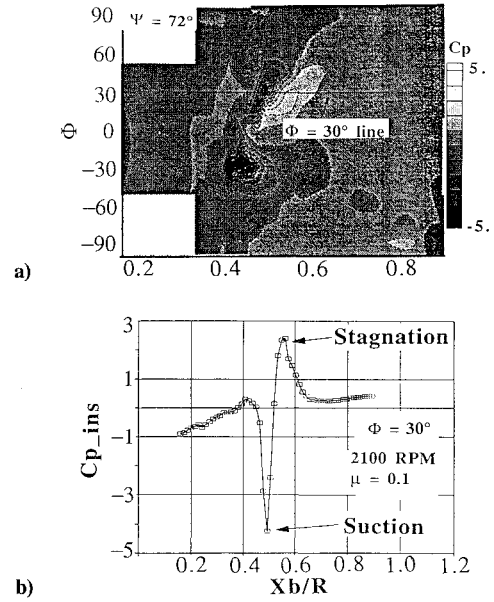


Fig. 9 a) Cylinder surface pressure distribution at $\Psi = 72$ deg and b) pressure variation along the $\Phi = 30$ -deg line.

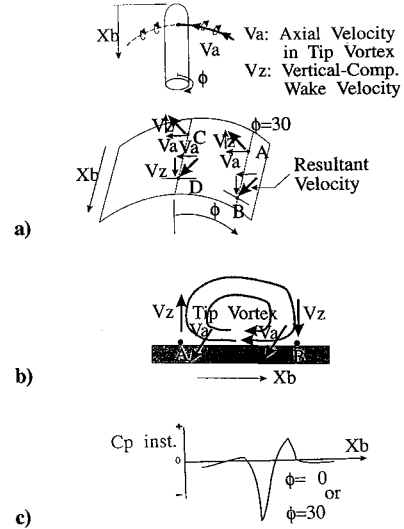


Fig. 10 Schematic vectorial interpretation of the stagnation of the vortex on the ABS of the GT cylinder.

axial component and the downward motion of the tip vortex in the downstream region are combined, the local incidence angle between the resultant velocity and the airframe surface on the ABS becomes closer to a right angle. However, when the axial component in the core is combined with an upward velocity at the upstream edge of the core, the incidence angle becomes smaller. The local pressure is maximum when the incidence is 90 deg.

Interaction with Separated Flow Regions

The preceding discussion has assumed that the flow over the cylinder is attached and unidirectional in the absence of the wake. However, on most rotorcraft configurations, regions of separated flow are common, such as behind the rotor hub, on the sides of the fuselage, and on the tail boom. A major uncertainty is the behavior of the rotor wake when interacting with such flows, which poses substantial computational difficulties. A study of this problem was completed,^{27,29} substituting a boom of smaller diameter for the aft portion of the GT cylinder, thereby creating a large, sharp-edged backward-facing step and recirculation region in the region of vortex interaction. The findings are summarized as follows: the tip vortex overpowers the recirculating flow region, so that the vortex interaction with the surface occurs in a manner essentially similar

to what happens when there is no flow separation. The separated flow region is periodically destroyed and recreated. Although the interaction appears complex, flow visualization and pressure spectral measurements reveal that the interaction can be modeled essentially as a linear superposition of a vortex sheet representing the separated free shear layer and the tip vortex. It is argued that the case studied, with a sharp-edged separation region, represents the highest ratio of shear-layer vorticity to tip vortex strength. At higher rotor advance ratios, where the sheet may be stronger, the tip vortex would pass over the region without significant interaction. Thus, it appears that the separated-flow interaction can be modeled quite simply without fear of first-order complications; the effect on the rotor wake is minimal.

Areas of Major Uncertainty

We now see that there are three major issues remaining in the vortex/airframe interaction. The first is the three-dimensional, unsteady boundary-layer interaction during and after vortex collision. This requires detailed, sophisticated experimental and computational approaches, since it deals with the largely unexplored area of unsteady, three-dimensional flow separation. The mechanics of vortex collision are also extremely complex, particularly due to the high energy of the vortex and the axial flow in its core. The second issue is thus the detailed modeling and measurement of the core structure of the vortex in forward flight, another major task. The third is an area avoided in this paper: that of compressibility in the vortex flow. This will certainly affect the two issues first mentioned, have significant effects on noise generation by vortex interaction, and probably influence flow separation due to shock/boundary-layer interaction.

Conclusions

Although much remains unknown about vortex-surface interactions in general and the rotor wake/airframe interaction in particular, several important advances have been made. It is now possible to generate physically correct models of the vortex behavior around the airframe. This removes a major uncertainty in the computation of rotorcraft aerodynamics. Specific aspects are as follows:

- 1) The interaction phenomena are basically different at the front and aft portions of the rotor wake, because of the opposite senses of vortex rotation.
- 2) The vortex trajectory is initially distorted as predictable from knowledge of the vortex strength and the flow over the airframe. The front vortex filament is decelerated and proceeds directly to collide with the surface, whereas the aft filament slides over the surface in a weaker grazing interaction. In the process, both the front and aft filaments stretch, the aft filament more than the front filament.
- 3) There is a strong axial velocity in the core of the tip vortex, directed wake-like toward the blade of vortex origin. From the few measurements available to date, the axial component is roughly the same order as the inflow velocity to the rotor plane for typical interaction parameters.
- 4) The vortex collision at the front is accompanied by local boundary-layer separation upstream of impact, followed by a sharp increase, a decrease, and then a rise in surface pressure.
- 5) Following collision, the remains of the filament at the top appear to merge with the boundary layer, its vorticity adding to that in the boundary layer.
- 6) The effect of this collision propagates along the filament on the RBS, so that a weaker vortex is seen on this side.
- 7) The surface pressure signature under the RBS is dominated by the vortex core suction pressure and the upstream boundary-layer separation.
- 8) The surface pressure signature under the ABS is characterized by the stagnation of the axial and azimuthal flow in the vortex core, as well as the low-pressure region during the phase of the encounter with a favorable flow orientation.
- 9) The vortex interaction effect leaves the surface before reaching the bottom on the RBS. The interaction extends to the bottom from the ABS and a little beyond. This asymmetry is due to the axial flow in the core.
- 10) The rolled-up edge of the inboard sheet, which rotates counter to the tip vortex, interacts with the surface in a manner that is

essentially opposite to that of the tip vortex, but with much weaker effects. This interaction diverges from the tip vortex interaction region at both the front, and (probably, not yet verified) at the aft regions.

11) There is substantial vortex unsteadiness prior to impact on the surface.

12) At the aft end, the filaments on either side are distorted by the sliding above the surface, but proceed without further surface interaction.

13) The presence of separated-flow regions does not significantly alter the physical nature of the vortex/airframe interaction because the strength of the vortex is much higher than that of any vorticity in the separated shear layer.

We emphasize, in closing, that this is a summary, meant to provide a way to model the wake/airframe interaction. The interaction process is rich in detail and complexity, with problems that are still at the leading edge of fluid mechanics research.

Acknowledgments

This work was sponsored by the Army Research Office under DAAL03-88-C-0003-AD2, Aerodynamics Task 2 of the Center of Excellence in Rotary Wing Aircraft Technology. T. L. Doligalski is the Technical Monitor. The contributions of the many researchers mentioned in this paper are gratefully acknowledged. In particular, the authors thank A. G. Brand, S. G. Liou, and A. T. Conlisk for valuable discussions on the physics of the problem, and John Lynn for assistance with the figure revisions.

References

- ¹Brand, A. G., Komerath, N. M., and McMahon, H. M., "Results from the Laser Sheet Visualization of an Incompressible Vortex Wake," *Journal of Aircraft*, Vol. 26, No. 5, 1989, pp. 438-443.
- ²Bagai, A., and Leishman, J. G., "Experimental Study of Rotor Wake/Body Interactions in Hover," *Journal of the American Helicopter Society*, Vol. 37, No. 4, 1992, pp. 48-57.
- ³Lorber, P. F., and Egolf, T. A., "An Unsteady Helicopter Rotor-Fuselage Interaction Analysis," NASA CR4178, 1988.
- ⁴Brand, A. G., Komerath, N. M., and McMahon, H. M., "Wind Tunnel Data from a Rotor Wake/Airframe Interaction Study," GITAER86-1, Contract DAAG29-82-K-0094, Georgia Inst. of Technology, Atlanta, GA, July 1986.
- ⁵Quackenbush, T. R., and Bliss, D. B., "Free Wake Calculation of Rotor Flow Fields of Interactional Aerodynamics," *Proceedings of the 44th Annual Forum of the American Helicopter Society*, Washington, DC, June 1988, pp. 29-43.
- ⁶Norman, T., and Light, J., "Rotor Tip Vortex Geometry Measurements Using the Wide-Field Shadowgraph Technique," *Journal of the American Helicopter Society*, Vol. 32, No. 2, 1987.
- ⁷Liou, S.-G., Komerath, N. M., and McMahon, H. M., "Measurement of Transient Vortex-Surface Interaction Phenomena," *AIAA Journal*, Vol. 28, No. 6, 1990, pp. 975-981.
- ⁸Mavris, D. M., Komerath, N. M., and McMahon, H. M., "Prediction of Rotor/Airframe Aerodynamic Interactions," *Journal of the American Helicopter Society*, Vol. 34, No. 4, 1989, pp. 37-46.
- ⁹Scully, M. P., "Computation of Helicopter Rotor Geometry and Its Influence on Rotor Harmonic Airloads," Massachusetts Inst. of Technology Aeroelastic and Structures Research Lab., Rept. ASRL TR 178-1, Massachusetts Inst. of Technology, Cambridge, MA, March 1975.
- ¹⁰Clark, D. R., "Study for Prediction of Rotor/Wake/Fuselage Interference: Parts I and II," NASA CR-16653-1 and II, Nov. 1983.
- ¹¹Komerath, N. M., Mavris, D. M., and Liou, S.-G., "Prediction of Unsteady Pressure and Velocity over a Rotorcraft in Forward Flight," *Journal of Aircraft*, Vol. 28, No. 8, 1991, pp. 509-516.
- ¹²Doligalski, T. (ed.), Abstracts of Proceedings of the First A.R.O. Workshop on Rotorcraft Interactional Aerodynamics, Army Research Office, Research Triangle Park, NC, July 1988.
- ¹³Light, J. S., Frekring, A. A., and Swanson, T. R., "Application of the Wide-Field Shadowgraph Technique to Helicopters in Forward Flight," *Journal of the American Helicopter Society*, Vol. 37, No. 2, 1992, pp. 23-28.
- ¹⁴Berry, J. D., "Prediction of Time-Dependent Fuselage Pressures in the Wake of a Helicopter Rotor," *Proceedings of the Eighth European Rotorcraft and Powered Lift Aircraft Forum*, Sept. 1992.
- ¹⁵Schreiber, O. A., "Aerodynamic Interactions Between Bodies in Relative Motion," Ph.D. Thesis, School of Aerospace Engineering, Georgia Inst. of Technology, Atlanta, GA, Aug. 1990.
- ¹⁶Cantaloube, B., and Huberson, S., "A New Approach Using Vortex Point Method for Prediction of Rotor Performance in Hover and Forward Flight," *9eme Forum Europeen d'Helicoptere*, Stresa, Sept. 1983.

¹⁷Clark, D. R., and Maskew, B., "A Re-examination of the Aerodynamics of Hovering Rotors Including the Presence of the Fuselage," *Proceedings of the International Technical Specialists' Meeting on Rotorcraft Basic Research*, Georgia Inst. of Technology, Atlanta, GA, 1991, pp. 40-1-40-13.

¹⁸Brand, A. G., McMahon, H. M., and Komerath, N. M., "Correlations of Rotor Wake/Airframe Interaction Measurements with Flow Visualization Data," *Journal of the American Helicopter Society*, Vol. 35, No. 4, 1990, pp. 4-15.

¹⁹Conlisk, A. T., "The Pressure Field in an Intense Vortex-Boundary Layer Interaction," AIAA Paper 89-0293, Jan. 1989.

²⁰Doligalski, T. L., and Walker, J. D. A., "The Boundary Layer Induced by a Convected Rectilinear Vortex," *Journal of Fluid Mechanics*, Vol. 139, 1984, pp. 1-30.

²¹Chuang, F. S., and Conlisk, A. T., "The Effect of Interaction on the Boundary Layer Induced by a Convected Rectilinear Vortex," *Journal of Fluid Mechanics*, Vol. 200, 1989, pp. 337-365.

²²Affes, H., and Conlisk, A. T., "A Simplified Model for the Interaction of a Rotor Tip Vortex With an Airframe," AIAA Paper 92-0320, Jan. 1992.

²³Affes, H., and Conlisk, A. T., "The Three-dimensional Boundary Layer

Flow Due to a Vortex Filament Outside a Circular Cylinder," AIAA Paper 93-0212, Jan. 1993.

²⁴Affes, H., Xiao, Z., Conlisk, A. T., Kim, J. M., and Komerath, N. M., "The Three-Dimensional Boundary Layer Flow Due to a Rotor Tip Vortex," AIAA Paper 93-3081, July 1993.

²⁵Affes, H., "Tip Vortex-Airframe Interactions," Ph.D. Thesis, Dept. of Mechanical Engineering, Ohio State Univ., 1992.

²⁶Thompson, T. L., Komerath, N. M., and Gray, R. B., "Visualization and Measurement of the Tip Vortex Core of a Rotor Blade in Hover," *Journal of Aircraft*, Vol. 25, No. 12, 1988, pp. 1113-1121.

²⁷Kim, J. M., "An Experimental Study of the Interaction Between a Rotor Wake and an Airframe With and Without Flow Separation," Ph.D. Thesis, School of Aerospace Engineering, Georgia Inst. of Technology, Atlanta, June 1993.

²⁸Kim, J. M., Komerath, N. M., and Liou, S.-G., "Vorticity Concentration at the Edge of the Inboard Vortex Sheet," *Journal of the American Helicopter Society*, Vol. 39, No. 2, 1994, pp. 30-34.

²⁹Komerath, N. M., Kim, J. M., and Liou, S.-G., "Rotor Wake Interaction with Separated Flow," *Mathematical and Computer Modelling*, Vol. 18, No. 3/4, 1993, pp. 73-87.

Recommended Reading from
Progress in Astronautics and Aeronautics

MECHANICS AND CONTROL OF LARGE FLEXIBLE STRUCTURES

J.L. Junkins, editor

This timely tutorial is the culmination of extensive parallel research and a year of collaborative effort by three dozen excellent researchers. It serves as an important departure point for near-term applications as well as further research. The text contains 25 chapters in three parts: Structural Mod-

eling, Identification, and Dynamic Analysis; Control, Stability Analysis, and Optimization; and Controls/Structure Interactions: Analysis and Experiments. 1990, 705 pp, illus, Hardback, ISBN 0-930403-73-8, AIAA Members \$69.95, Nonmembers \$99.95, Order #: V-129 (830)

Place your order today! Call 1-800/682-AIAA



American Institute of Aeronautics and Astronautics

Publications Customer Service, 9 Jay Gould Ct., P.O. Box 753, Waldorf, MD 20604
FAX 301/843-0159 Phone 1-800/682-2422 8 a.m. - 5 p.m. Eastern

Sales Tax: CA residents, 8.25%; DC, 6%. For shipping and handling add \$4.75 for 1-4 books (call for rates for higher quantities). Orders under \$100.00 must be prepaid. Foreign orders must be prepaid and include a \$20.00 postal surcharge. Please allow 4 weeks for delivery. Prices are subject to change without notice. Returns will be accepted within 30 days. Non-U.S. residents are responsible for payment of any taxes required by their government.